

Development and Experimental Verification of a Mathematical Model of Lithium Ion Battery

D. A. Bograchev^a, Yu. M. Vol'fkovich^a, V. S. Dubasova^b, A. F. Nikolenko^b,
T. A. Ponomareva^b, and V. E. Sosenkin^{a, z}

^a*Frumkin Institute of Physical Chemistry and Electrochemistry, Russian Academy of Sciences,
Leninskii pr. 31, Moscow, 119071 Russia*

^b*Scientific Research Institute of Electrical Carbon Products, Moscow oblast', Elektrougli, 142455 Russia*

Received July 21, 2011

Abstract—A model of the lithium ion battery is developed which takes into account intercalation and extraction of lithium ions in the active mass of negative and positive electrodes, the dependences of equilibrium electrode potentials on the concentration of intercalated lithium, the ion transfer in pores of electrodes and the separator, the kinetics of electrode reactions, and the electric double layer charging. As the active material for the negative electrode, UAMS graphite material is used. Lithium-nickel-cobalt oxide serves as the positive electrode. The porous structure of electrodes is studied by the method of standard contact porosimetry. Sufficiently high porosity values found for both electrodes (50% for anode and 27% for cathode) made it possible to consider the interface as regards the internal pore surface found from porosimetry data rather than as regards their external surface as in the previous studies. A comparison of calculated and experimental discharge curves demonstrates their closeness, which points to the correctness of the model. By the fitting procedure, the coefficients of solid-state diffusion of lithium ions and the rate constants for reactions on both electrodes are found.

Keywords: lithium-ion batteries, intercalation, extraction, lithium-nickel-cobalt oxide, graphite, porosimetry, solid-state diffusion, mathematical simulations, electric double layer

DOI: 10.1134/S1023193513020031

INTRODUCTION

The development of batteries that employ intercalation of lithium ions was initiated in the 70s of the past century [1] and merely twelve years later, a Japanese company Sony started to sell commercial lithium-ion rechargeable batteries [2] based on the same principle. Lithium ion batteries have quickly occupied the leading position in the market of batteries for mobile devices because they displayed the following significant advantages over traditional rechargeable batteries; a comparatively high accumulated energy density, the absence of “memory” effect, high cyclability, the possibility of creating batteries of various shapes and sizes and with exhibiting higher open circuit voltage values as compared with aqueous systems, etc. [3].

The batteries developed had their drawbacks, namely, the comparatively short lifetime, the high inner resistance, the probability of formation of metal Li under overcharging conditions or at negative temperatures. To understand these processes and optimize the device operation, an adequate model was required. The first model of this kind was developed by Newman [4]. It deserves mention that the problem of modeling individual porous electrodes with intercalation was

posed earlier, for instance, a model of porous intermetallic electrodes, i.e., hydrogen adsorbents, was developed [5] and used later for electrodes based on electron-conducting polymers in which intercalation of counter ions occurred [6, 7].

The Newman model was used in optimizing the structure [8] and served the basis for the development of various other models, namely, from those taking into account heat effects [9, 10], relaxation processes [11], and the electric double layer (EDL) capacitance [12] to those describing the decay of electric characteristics at cyclic operation of the battery [13–15]. This model was also used in the analysis of impedance data, working characteristics, and transition processes in batteries [16–18].

The approach to modeling the lithium-ion batteries was based on the use of the theory of transfer in porous media [19] developed for electrochemical systems [20, 21] and the theory of intercalation processes in electrodes [22]. Mention should be made of the studies devoted to modeling lithium cells which consider the percolation effects [23, 24].

The majority of models (ignoring heat liberation) followed the result of [4] and adopted the “sandwich” geometry (Fig. 1). In figure, the positive electrode

^z Corresponding author: vsosenkin@mail.ru (V.E. Sosenkin).

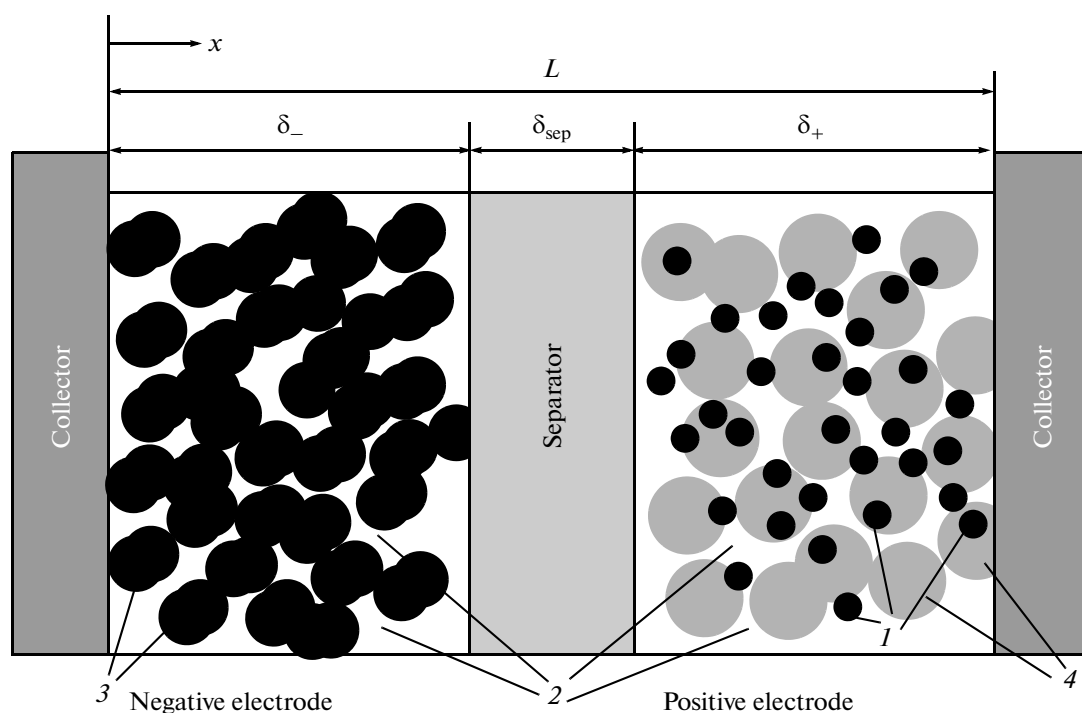


Fig. 1. Illustration of a battery: (1) conductive additive; (2) pores, (3) porous NE grains, (4) porous PE grains.

(PE) is on the right (it serves as the source of Li^+ ions at cell charging), the negative electrode (NE) is on the left (it serves the source of Li^+ ions at the cell discharge); between them, a porous separator is placed, which eliminates the electron conductivity between NE and PE.

The model illustrated in Fig. 1 is often called the pseudo 2D-model, having, in fact, the following two dimensions: the macrolevel dimension corresponding to that of concentration and potential distributions over the thickness of electrodes and separator and also the microlevel dimension corresponding to intercalation in particles of the electrode active mass.

For microlevel modeling, the porous electrode structure is considered as built of closely packed spherical grains of equal radii on the surface of which the process of intercalation–extraction of lithium ions governed by Butler–Volmer kinetics occurs. In models of batteries, the solid-state diffusion coefficient is assumed to be independent of concentration, although these systems are known to demonstrate certain deviations from the Fick law [25, 26]. The electron conductivity of electrodes is assumed to be independent of the concentration of intercalated lithium and the dependence of the quasi-equilibrium electrode potential on the concentration is taken directly from low-current experiments.

To combine micro- and macrolevels, it is assumed that each point throughout the electrode thickness corresponds to a certain microparticle and, the other

way round, each microparticle in electrodes is located in a certain point throughout the electrode thickness. This assumption implies that the characteristic electrode thickness much exceeds the diameter of constituent particles; however, this is not strictly fulfilled in all cases. Among the known literature data (e.g., [11]), the particles size and the thickness differ only 5-fold for NE.

The transfer of ions in model [4] is primarily described by equations for concentrated electrolytes; however, in fact, because the parameters are unknown, the approximation with independency of the diffusion coefficient of concentration was used. The experimental bell-shaped dependence of the electrolyte conductivity on concentration was used only in calculating the ohmic potential drop.

The system of equation describing intercalation and diffusion in a porous medium and the electric field distribution in the electrolyte and the solid phase during the lithium-ion cell operation is severely non-linear and its analytical solution can be found only for the limiting cases [27].

For the numerical solution of the system of equations describing the process of discharge of a lithium-ion battery, different approaches were used, which were mainly based on the method of finite differences [4, 28]. The numerical methods for solution are surveyed in [29].

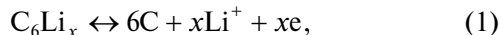
In the present study, we used the method of finite elements solving numerically the equations of this

model. The calculated charge-discharge curves were compared with experimental curves. By fitting the model to experimental data, the kinetic parameters of reaction and the solid-phase diffusion coefficients were calculated.

THEORETICAL ANALYSIS

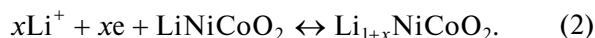
As was mentioned above, the model shown in Fig. 1 consists of three elements: a composite NE (LiC_6), an electrolyte-filled separator, and a composite PE ($\text{LiNi}_{0.8}\text{Co}_{0.2}\text{O}_2$).

The following reaction proceeds on NE:



where x is 1 at complete charging.

On PE, the following reaction proceeds:



During the discharge, lithium ions diffuse in the solid phase from the bulk to the surface of LiC_6 particles (the process of extraction in the negative electrode) and then pass to electrolyte solution (or gel) taking part in the electrochemical reaction. Lithium ions are transferred by the diffusion-migration mechanism from NE pores to pores in the separator and then to PE pores. After the electrochemical reaction on the surface of PE particles, lithium ions diffuse in the solid phase inside these particles (the intercalation process). In calculations, the NE and PE particles are considered as globules for simplicity sake, although according to the electron scanning microscopy data, NE particles are shaped as flakes or porous spheres and PE grains are shaped as globules built of single crystals.

We follow the results of studies [8, 30] in which equations describing the work of a lithium battery were derived within the approximation of porous electrode macrokinetics.

Assume that lithium transfer in particles is described by the Fick law

$$\frac{\partial c}{\partial t} = \frac{D_s}{r^2} \frac{\partial}{\partial r} \left(r^2 \frac{\partial c_s}{\partial r} \right) \quad (3)$$

with boundary conditions

$$\left. \frac{\partial c_s}{\partial r} \right|_{r=0} = 0, \quad (4)$$

$$D_s \left. \frac{\partial c_s}{\partial r} \right|_{r=R_s} = \frac{-j^{\text{Li}}}{S_e F}, \quad (5)$$

where D_s is the solid-phase diffusion coefficient, c_s is the concentration of lithium in the solid phase, r is the current radius of particles, $R_s = 3(1 - \varepsilon_e)/S_e$ is the average radius of particles, j^{Li} is the volume current of the electrochemical reaction on a porous surface which represents divergence of the vector of current density throughout the electrode volume and, correspond-

ingly, has the dimension of A/cm^3 ($j^{\text{Li}} > 0$ corresponds to electrode discharge); ε_e is the electrode porosity, F is the Faraday number.

The specific surface area was calculated based on data obtained by the BET method and also by the method of standard contact porosimetry [31, 32]. According to the latter

$$S_e(r_{\text{por}}) = 2 \int_{r_{\text{min}}}^{r_{\text{max}}} \frac{dv}{dr_{\text{por}}} \frac{dr_{\text{por}}}{r_{\text{por}}}. \quad (6)$$

Where dv/dr_{por} is the differential function of distribution of pore volume v over radii r_{por} .

Transfer of lithium ions in electrolyte is described sufficiently well by the following equation [4, 8]:

$$\varepsilon_e \frac{\partial c_e}{\partial t} = \frac{\partial}{\partial x} \left(D_e^{\text{eff}} \frac{\partial c_e}{\partial x} \right) + \frac{1-t_+^0}{F} (j^{\text{Li}} + j^{\text{C}}) \quad (7)$$

with zero (insulating) boundary conditions on collectors

$$\left. \frac{\partial c_e}{\partial x} \right|_{x=0} = \left. \frac{\partial c_e}{\partial x} \right|_{x=L} = 0, \quad (8)$$

where c_e is the effective electrolyte concentration, t_+^0 is the transport number of lithium ions in the given electrolyte, D_e^{eff} is the effective diffusion coefficient of ions in electrolyte, j^{C} is the volume current of EDL charging.

The charge transfer in the solid phase can be found with the use of the divergence form of the Ohm law describing the potential distribution in this phase

$$\frac{\partial}{\partial x} \left(\sigma_e^{\text{eff}} \frac{\partial \varphi_s}{\partial x} \right) - (j^{\text{Li}} + j^{\text{C}}) = 0 \quad (9)$$

with boundary conditions on current collectors

$$-\sigma_-^{\text{eff}} \left. \frac{\partial \varphi_s}{\partial x} \right|_{x=0} = \sigma_+^{\text{eff}} \left. \frac{\partial \varphi_s}{\partial x} \right|_{x=L} = \frac{I}{A} \quad (10)$$

and zero boundary conditions on the separator

$$-\sigma_-^{\text{eff}} \left. \frac{\partial \varphi_s}{\partial x} \right|_{x=\delta_-} = \sigma_+^{\text{eff}} \left. \frac{\partial \varphi_s}{\partial x} \right|_{x=L-\delta_+} = 0, \quad (11)$$

where φ_s is the potential in the solid phase, σ_e^{eff} is the solid phase conductivity, I is the total current, A is the surface area of cell's electrodes, δ_- and δ_+ are the thicknesses of NE and PE, respectively.

The law of transfer in electrolytes is expressed in a more complicated form as compared with Eq. (9)

$$\frac{\partial}{\partial x} \left(k^{\text{eff}} \frac{\partial \varphi_e}{\partial x} \right) + \frac{\partial}{\partial x} \left(k_D^{\text{eff}} \frac{\partial \ln c_s}{\partial x} \right) + (j^{\text{Li}} + j^{\text{C}}) = 0, \quad (12)$$

where the boundary conditions are the absence of current on collectors

$$\left. \frac{\partial \varphi_e}{\partial x} \right|_{x=0} = \left. \frac{\partial \varphi_e}{\partial x} \right|_{x=L} = 0, \quad (13)$$

where φ_e is the electric potential in electrolyte, k^{eff} is the effective coefficient of electrolyte conductivity in a porous medium, determined based on Archie's law $k^{\text{eff}} = k_0 \varepsilon_e^{1.5}$. The coefficient k_D^{eff} can be found in terms of the dilute electrolyte theory as

$$k_D^{\text{eff}} = \frac{2RTk^{\text{eff}}}{F} (t_+^0 - 1) \left(\frac{\partial \ln f_{\pm}}{\partial \ln c_e} \right), \quad (14)$$

where f_{\pm} is the activity coefficient taken constant in the given model, R is the gas constant, T is the temperature. The kinetic equation of the electrochemical interface reaction is the Butler–Volmer equation (slow discharge theory)

$$j^{\text{Li}} = S_e i_0 \left[\exp\left(\frac{\alpha_a F}{RT} \eta\right) - \exp\left(-\frac{\alpha_c F}{RT} \eta\right) \right], \quad (15)$$

where α_a and α_c are the transfer coefficients in the anodic and cathodic reactions, i_0 is the exchange current density, η is overpotential representing the potential difference between the solid phase and electrolyte minus the thermodynamic equilibrium potential

$$\eta = \varphi_s - \varphi_e - U(c_{s,e}), \quad (16)$$

where $U(c_{s,e})$ is represented as a tabulated function of the lithium concentration on the particle surface (usually approximated by a certain polynomial individual for each material). The exchange current density is set [4, 8] as follows:

$$i_0 = k^r (c_{s,\text{max}} - c_{s,e})^{\alpha_a} c_{s,e}^{\alpha_c} c^{\alpha_c}, \quad (17)$$

where k^r is the reaction rate constant, $c_{s,\text{max}}$ is the maximum (as regards stoichiometry) lithium concentration in the electrode solid phase. The equation describing the EDL charging is as follows:

$$j^c = S_e C \frac{\partial(\varphi_e - \varphi_s)}{\partial t}, \quad (18)$$

where C is the EDL capacitance.

Finally, the measured voltage of the cell can be represented as follows:

$$V = \varphi_s|_{x=L} - \varphi_s|_{x=0} - \frac{I}{A} R_f, \quad (19)$$

where R_f is the total contact resistance.

EXPERIMENTAL

To verify the model experimentally, we prepared positive and negative electrodes and subjected them to electrochemical tests in both half-cells with lithium counter electrodes and within batteries.

The NE active material represented the UAMS graphite material based on Russian natural flaked graphite from the Taiginskoe graphite deposit. This material was treated mechanically and thermally (NIIEI). For PE, a mixed lithium–nickel–cobalt oxide (Baltiiskaya Manufactura) was used. The NE

was prepared by the deposition of the electrode mass containing the mentioned carbon material, a polymer binder, and a solvent onto copper foil. An aqueous suspension of butadiene–nitrile latex in water served as the binder. For PE, polyvinylidene fluoride was taken as the binder and N-methylpyrrolidone served as the solvent. The PE active mass additionally contained a conducting additive (technological carbon). After thorough mixing with a magnetic stirrer, the active electrode mass was spread over the copper foil (for NE) or aluminum foil (for PE) by mean of a spreading unit. Foil with the deposited mass was preliminarily dried by broaching through the furnace of the spreading unit. Then, the roll with the coating was cut to electrode workpieces and the latter were vacuum dried for 15 h at 360 K. From the dried workpieces, electrodes of required size were cut by cutting dies. To provide the necessary density of the electrode layer, the dried and cut electrodes were passed through a HSNE-1t roll press and rolled to the required thickness.

For experimental checkup, NE and PE samples with tabulated parameters were prepared.

For electrochemical tests of electrodes under study, we assembled either half-cells for each studied electrode, which also contained a lithium counter electrode, or batteries containing both electrodes under study. Half-cells were assembled in fluoropolymer electrochemical cells with the cylindrical space 1 cm in diameter. Prepared electrodes shaped as disks with the surface of 3.1 cm² were sealed in a polypropylene–polyethylene–polypropylene separator manufactured by Celgard and then dried in vacuum for 15 h at 350 K before being fixed in the cells. A tested electrode was placed into a cell between two lithium counter electrodes and then the cell was filled with electrolyte. All operations on preparation of lithium electrodes, assembling of electrochemical cells and their filling were carried out in glove boxes in the dry argon atmosphere. As the electrolyte, 1 M LiPF₆ solution in the equimolar mixture of ethylene carbonate, dimethyl carbonate, and methylethyl carbonate was used.

To test the studied electrodes within batteries, small prismatic batteries corresponding to the ICNP size of 11/35/50 were used. They included a stainless steel case with the overall dimensions of (10.5 × 32.5 × 47.5), a lid with the pressure seal for the PE and the orifice for pouring electrolyte, and the electrode assembly. The electrode assembly consisted of NE and PE divided by a separator and rolled into an elliptic roll with positive and negative collectors. Electrolyte was poured in a special “dry” box by using a filling setup after the preliminary evacuation. After pouring electrolyte, the battery was assembled on a multichannel automatic charge–discharge complex 10 UZR-30mA-10V; the procedure involved the battery charging up to voltage of 4.2 V first under galvanostatic conditions with the current of 280 mA and then under potentiostatic conditions at descending current up to the final value of 55 mA.

To assess the dependences of the quasi-equilibrium potential for each electrode under study on the lithium concentration, the measurements were carried out in half-cells under galvanostatic conditions with small currents (0.5 mA) corresponding to the charge and discharge rates of $(0.04\text{--}0.05) C_{\text{nom}}$. At the anodic and cathodic polarization of tested electrodes in half-cells, the potential difference between the tested electrode and interconnected lithium counter electrodes was measured. Insofar as in the initial stage of tests (in the absence of long-term cycling) at the current densities used in this study, the potentials of fresh lithium counter electrodes differed insignificantly from the potential of the reversible lithium electrode, this potential difference can be assumed as a potential with respect to the reversible lithium electrode within to acceptable error. The NE characteristics were studied in the working potential range from 0.02 to 1.0 V; the PE characteristics were studied in the range from 4.3 to 3.0 V. In the battery tests, the voltage on collectors was measured.

The capacity characteristics of batteries with electrodes under study were assessed at different discharge currents, the measurements were carried out in several consecutive cycles differing in the discharge current at one and the same charging mode. The battery charging was carried out in two steps: at the constant current of 260 mA equal to $0.2 C_{\text{nom}}$ up to the voltage of 4.2 V and then in the descending current mode up to 40 mA. The discharge in each cycle was carried out in galvanostatic mode with the current of 0.28, 0.56, 0.84, 1.12, and 1.4 A.

The tests were carried out on an automatic test bench Atlas, which made it possible to set the current magnitude and direction, the duration of individual stages and also to control and measure current, voltage, time, and capacity during the tests.

Porosimetric measurements were carried out by the method of standard contact porosimetry (SCP) [31, 32]. This method allows the distribution of curves over the pore radius to be measured in the maximum wide range of radii (from 0.3 to 3×10^5 nm, i.e., in an interval of 6 orders of magnitude. Moreover, in contrast to the widely known method of mercury porosimetry, it allows the amalgamated and easily compressible materials and samples to be investigated. In our case, this was important because we used copper foil as the current collector for NE. As the measuring liquid, octane which wets any material was used.

RESULTS AND DISCUSSION

Figure 2 shows the integral (a) and differential (b) SCP curves describing the pore volume distribution over radii for NE and PE. From these figures, the following conclusion can be drawn: (a) the NE porosity (50%) is almost double that of PE (27%); (b) the main

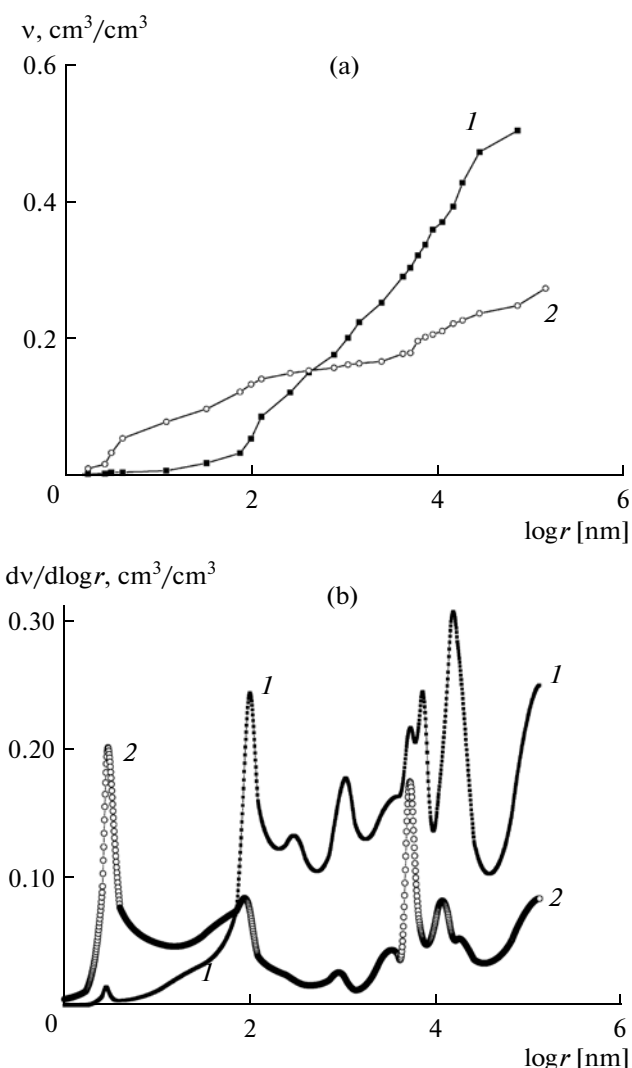


Fig. 2. (a) Integral and (b) differential curves of pore volume distribution over radii for (1) NE and (2) PE.

volume of pores falls to the range of their radii from 30 to 5×10^5 nm for NE and from 3 to 5×10^5 nm for PE; thus, the pore radius intervals for both electrodes are very wide, of 4–5 orders; (b) the high porosity values for both electrodes provide the grounds for considering the model interface as regards the inner surface of pores calculated from porosimetry data rather than as regards the external surface of grains as in [4, 8]. Based on these curves and Eq. (6), the following values were found for the NE specific surface area: $7.2 \text{ m}^2/\text{g}$ or $6.5 \text{ m}^2/\text{cm}^3$. For the PE active mass, the specific surface area ($0.6 \text{ m}^2/\text{g}$ or $1.74 \text{ m}^2/\text{cm}^3$) was found by the BET method. The analogous values could be hardly obtained based on the porosimetric curves shown above, because the composition of studied electrodes includes components (carbon black and binder) other than the active mass.

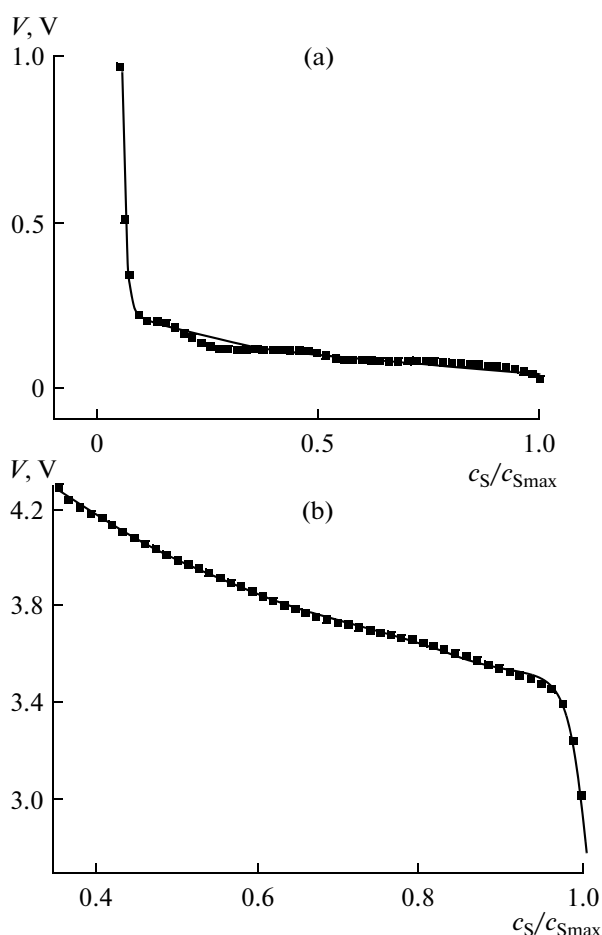


Fig. 3. Quasi-equilibrium potential of (a) NE and (b) PE as a function of lithium concentration. Points correspond to experiments; solid line corresponds to calculations with approximating function.

To simulate the work of a battery, it is necessary to know the dependence of the electrolyte conductivity on the concentration and the dependence of the quasi-equilibrium electrode potential on their degree of intercalation. We took the semi-empirical bell-shaped dependence of conductivity, similar to that used in [4, 8], with the maximum at 0.8 S/m at 1 M concentration.

The experimentally found quasi-equilibrium electrode potentials as a function of the dimensionless concentration of lithium shown in Fig. 3 were measured at small currents.

When solving the equations of the model, the charged battery state was taken as the initial state for which the lithium filling was 99% for NE and 35% for PE. The time step was taken such that the discharge time was not lower than 5000 counts. The system behaved steadily with the exception of the last segment in which the polarization curve sharply bent and required smaller measuring steps.

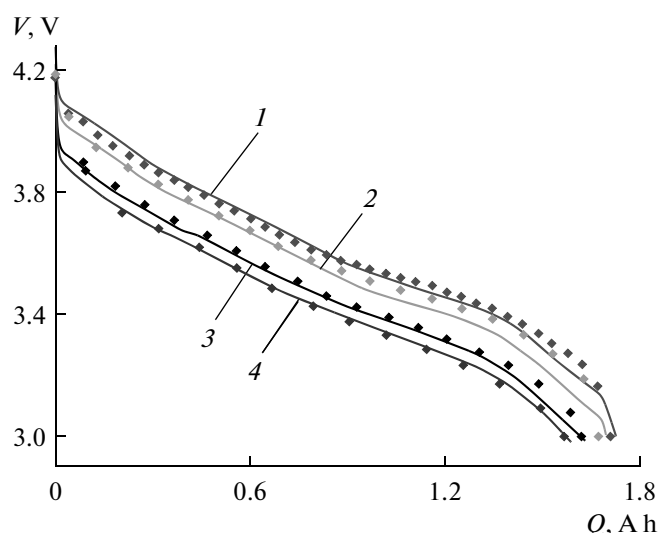


Fig. 4. Comparison of experimental (points) and calculated (lines) curves for a battery, obtained for different discharge currents, A: (1) 0.26, (2) 0.58, (3) 1.12, (4) 1.4.

In calculating the model discharge curves, it was assumed that the initial voltage depends on the reaction rate constant, while the position of the final bend in discharge curves is determined by the solid state diffusion coefficients. By varying the reaction rate constants and diffusion coefficients, it is possible to carry out the fitting procedure and attain coincidence between experimental and calculated curves.

Figure 4 shows the result of fitting of discharge curves. It is seen that the coincidence with experiment is sufficiently good, which points to correctness of the model. Table shows the calculated rate constants and also the coefficients of solid state diffusion and the parameters we used.

It deserves mention that the found diffusion coefficients are lower than reference data [4, 8]. We associated this with the fact that in [4, 8], porosimetric data were not taken into account in calculating the electrode particle size.

Figure 5 shows the profiles of dimensionless concentration of intercalated lithium for NE and PE up to the end of discharge when the voltage falls to 3 V. The vertical axis corresponds to dimensionless lithium concentration, the horizontal axes correspond to the dimensionless current radius of globules and their position with respect to the left edge of the electrode (Fig. 1). Based on these figures, it is evident that as the discharge current increases, the heterogeneity of the profile with respect to the globule radius also increases. This heterogeneity is most pronounced for PE with the lower lithium diffusion coefficient.

Parameters used in modeling the battery discharge

Parameter	Value	Source
Apparent surface area of electrodes, m^2	544×10^{-4}	Experiment
Exchange coefficient of PE and NE	0.5	Accepted
Solid-state diffusion coefficient of Li in PE, m^2/s	3.5×10^{-16}	Fitting
Solid-state diffusion coefficient of Li in NE, m^2/s	4×10^{-15}	Fitting
Diffusion coefficient of Li in electrolyte, m^2/s	5.25×10^{-11}	[4, 8]
Transport number of Li	0.363	[4, 8]
Limiting concentration of lithium ions in PE, mol/m^3	4.4×10^4	Based on stoichiometry
Limiting concentration of lithium in NE, mol/m^3	3.15×10^4	Based on stoichiometry
PE Porosity, %	27	Experiment
NE Porosity, %	50	Experiment
Archie exponent for both electrodes	1.5	Accepted
Archie exponent for separator	1.5	Accepted
Separator porosity, %	50	Experiment
Specific surface of PE active mass, m^{-1}	1.74×10^6	Experiment
Specific surface of NE active mass, m^{-1}	6.5×10^6	Experiment
Average radius of particles of PE active mass, m	1.26×10^{-6}	Calculated base on experimental data
Average radius of particles of NE active mass, m	2.3×10^{-7}	Calculated base on experimental data
PE Conductivity, S/m	0.08	Experiment
NE Conductivity, S/m	9.73	Experiment
PE Active layer thickness, m	60×10^{-6}	Experiment
NE Active layer thickness, m	83×10^{-6}	Experiment
Separator thickness, m	25×10^{-6}	Experiment
Reaction rate constant on PE, $(\text{A m}^{2.5})/\text{mol}^{1.5}$	2×10^{-8}	Fitting
Reaction rate constant on NE, $(\text{A m}^{2.5})/\text{mol}^{1.5}$	8×10^{-8}	Fitting
Electric double layer capacitance, F/cm^2	20×10^{-6}	Accepted
Total contact resistance, Ω	0	Accepted

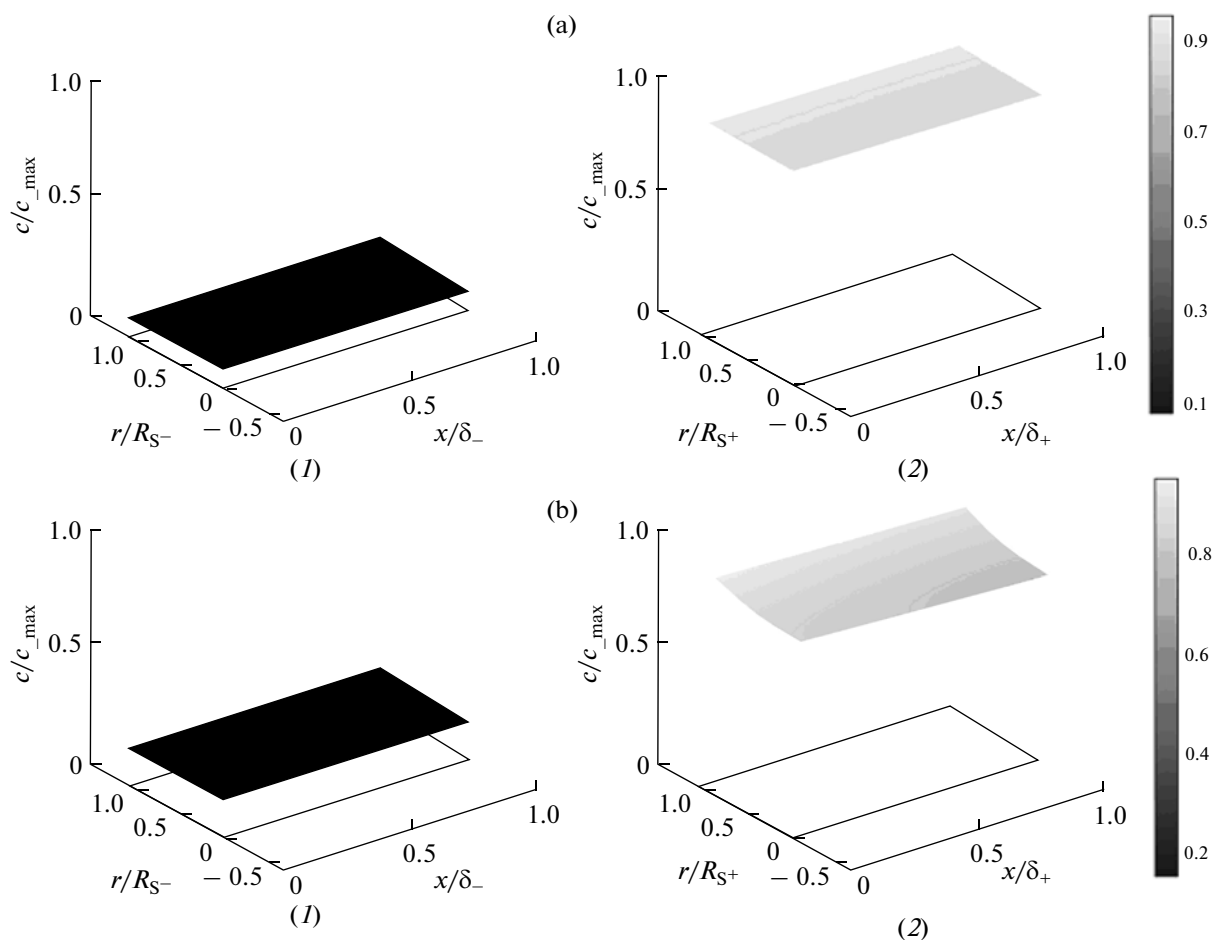


Fig. 5. Dimensionless profile of concentration of intercalated lithium ions in (1) NE and (2) PE globules for discharge currents of (a) 0.28 and (b) 1.4 A up to voltage of 3.0 V.

CONCLUSIONS

A model of the lithium-ion battery is developed which takes into account the processes of lithium ion intercalation and extraction in the NE and PE active mass, the dependences of quasi-equilibrium electrode potentials on the concentration of intercalated lithium, the processes of ion transport in pores of electrodes and separator, the kinetics of electrode reactions, the EDL charging, and the characteristics of the porous structure of electrodes and separator.

The porous structure was studied by the method of standard contact porosimetry. The NE porosity (50%) was almost double that of PE (27%). The main pore volume was in the range of their radii from 30 to 5×10^5 nm for NE and from 3 to 5×10^5 nm for PE. Thus, the pore radius ranges for both electrode were very wide comprising 4–5 orders of magnitude. The high porosity values for both electrodes provided the grounds for considering the interface in this model not as regards the external surface of grains as in earlier studies but as regards their internal surface calculated based on porosimetric data.

Discharge curves for individual electrodes and the whole battery were measured.

A comparison of calculated and experimental discharge curves demonstrated their closeness, which confirmed the correctness of this model. The fitting procedure afforded the solid-state diffusion coefficients for lithium ions and also the reaction rate constants for both electrodes.

The found diffusion coefficients were lower than reference data. This was attributed to the ignorance of porometric data when determining the size of pore-free electrode particles, due to which the globule size was overestimated in the cited studies [4, 8].

REFERENCES

1. Whittingham, M.S., *Electrical Energy Storage and Intercalation Chemistry*, Science, 1976, vol. 192, p. 1126.
2. Takehara, Z., *J. Power Sources*, 1989, vol. 26, p. 257.
3. Broussely, M., Biensan, P., and Simon, B., *Electrochim. Acta*, 1999, vol. 45, p. 3.

4. Doyle, M., Fuller, T., and Newman, J., *J. Electrochem. Soc.*, 1993, vol. 140, p. 1526.
5. Vol'fkovich, Yu.M., Petrii, O.A., Zaitsev, A.A., and Kovrigina, I.V., *Vestn. Mosk. Univ., Ser. 2: Khim.*, 1988, vol. 29, p. 173.
6. Volfkovich, Y.M., Bagotzky, V.S., Zolotova, T.K., and Pisarevskaya, E.Y., *Electrochim. Acta*, 1996, vol. 41, p. 1905.
7. Volfkovich, Y.M., Sergeev, A.G., Zolotova, T.K., Afanasiev, S.D., Efimov, O.N., and Krinichnaya, E.P., *Electrochim. Acta*, 1998, vol. 44, p. 1543.
8. Fuller, T.F., Doyle, M., and Newman, J., *J. Electrochem. Soc.*, 1994, vol. 141, p. 1.
9. Chen, Y. and Evans, J.W., *J. Electrochem. Soc.*, 1996, vol. 143, p. 2708.
10. Chen, Y. and Evans, J.W., *Electrochim. Acta*, 1994, vol. 39, p. 517.
11. Fuller, T.F., Doyle, M., and Newman, J., *J. Electrochem. Soc.*, 1994, vol. 141, p. 982.
12. Ong, I.J. and Newman, J., *J. Electrochem. Soc.*, 1999, vol. 146, p. 4360.
13. Kumaresan, K., Guo, Q., Ramadass, P., and White, R.E., *J. Power Sources*, 2006, vol. 158, p. 679.
14. Ploehn, H.J., Ramadass, P., and White, R.E., *J. Electrochem. Soc.*, 2004, vol. 151, p. 456.
15. Ramadass, P., Ploehn, H.J., and White, R.E., *Electrochem. Soc. Interface*, 2003, vol. 12, p. 65.
16. Smith, K. and Wang, C.Y., *J. Power Sources*, 2006, vol. 161, p. 628.
17. Bernardi, D.M. and Go, J.Y., *J. Power Sources*, 2011, vol. 196, p. 412.
18. Smith, K.A., Rahn, C.D., and Wang, C.Y., *Energy Conversion and Management*, 2007, vol. 48, p. 2565.
19. Bird, R.B., Stewart, W.E., and Lightfoot, E.N., *Transport Phenomena*, New York: Wiley, 1960.
20. Chizmadzhev, Yu.A., Markin, V.S., Tarasevich, M.R., and Chirkov, Yu.G., *Makrokinetika protsessov v poristykh sredakh* (Macrokinetics of Processes in Porous Media), Moscow: Nauka, 1971.
21. Newman, J. and Tiedemann, W., *AIChE J.*, 1975, vol. 21, p. 25.
22. Verbrugge, M.W. and Koch, B.J., *J. Electrochem. Soc.*, 1996, vol. 143, p. 24.
23. Chirkov, Yu.G., Rostokin, V.I., and Skundin, A.M., *Russ. J. Electrochem.*, 2011, vol. 47, p. 288.
24. Chirkov, Yu.G., Rostokin, V.I., and Skundin, A.M., *Russ. J. Electrochem.*, 2011, vol. 47, p. 299.
25. Verbrugge, M.W. and Koch, B.J., *J. Electrochem. Soc.*, 1996, vol. 143, p. 600.
26. Verbrugge, M.W. and Koch, B.J., *J. Electrochem. Soc.*, 1999, vol. 146, p. 833.
27. Doyle, M. and Newman, J., *J. Appl. Electrochem.*, 1997, vol. 27, p. 846.
28. Mao, Z. and White, R.E., *J. Electrochem. Soc.*, 1994, vol. 141, p. 151.
29. Botte, G.G., Subramanian, V.R., and White, R.E., *Electrochim. Acta*, 2000, vol. 45, p. 2595.
30. Doyle, M. and Newman, J., *J. Power Sources*, 1995, vol. 54, p. 46.
31. Volfkovich, Y.M. and Bagotzky, V.S., *J. Power Sources*, 1994, vol. 48, p. 327.
32. Volfkovich, Y.M., Bagotzky, V.S., Sosnenkin, V.E., and Shkolnikov, E.I., *Soviet Electrochem.*, 1980, vol. 16, p. 1325.